

PDF hosted at the Radboud Repository of the Radboud University Nijmegen

The following full text is a publisher's version.

For additional information about this publication click this link.

<http://hdl.handle.net/2066/35357>

Please be advised that this information was generated on 2020-11-26 and may be subject to change.

Stability of the polar {111} NaCl crystal face

Neda Radenović, Daniel Kaminski, Willem van Enckevort, Sander Graswinckel, Ismail Shah, Mendel in 't Veld, Rienk Algra, and Elias Vlieg^{a)}
IMM Solid State Chemistry, Radboud University Nijmegen, Toernooiveld 1, 6525 ED Nijmegen, The Netherlands

(Received 12 December 2005; accepted 14 February 2006; published online 25 April 2006)

We present a surface x-ray diffraction determination of the {111} NaCl-liquid interface structure. Using ultrathin water or formamide liquid layers we ascertained that the crystal surface is smooth at an atomic level and is not reconstructed. Our results reveal surprisingly small differences in surface structure between the two cases, which nevertheless lead to dramatic differences in crystal morphology. We determined that the rocksalt {111} surface is Na⁺ terminated for both environmental conditions. A quarter to half a monolayer of laterally disordered Cl⁻ ions is located on top of a fully ordered Na⁺ crystal surface with occupancy 0.75–1.0. This means that the polar surface is stabilized through the formation of an electrochemical double layer. © 2006 American Institute of Physics. [DOI: 10.1063/1.2185621]

I. INTRODUCTION

It is well known that impurities can have a large effect on crystal morphology. A variety of studies have been reported on mostly qualitative observations of morphological changes caused by the addition of small quantities of impurity.¹ However, the atomic-scale mechanism behind these effects is usually not known. The earliest report of a habit modifier is probably from Rome de l'Isle who reported the morphology transition from cubes to octahedrons if rock-salt is grown in the presence of urea,² i.e., the stable crystallographic face of NaCl changes from {100} to {111}. We have found that the addition of at least 20 wt % of formamide to the aqueous growth solution has the same effect.^{3,4}

This transition from the common {100} face to the octahedral or {111} face is an intriguing process, because the polar {111} face is not expected to be stable. Along the [111] direction the NaCl crystal consists of alternating layers of cations and anions. The resulting long-range electrostatic interactions lead to a very high energy of the {111} NaCl surface. Therefore, these polar surfaces should be highly unstable and not present in the morphology of NaCl-type crystals.⁵ Theoretical calculations for ionic crystals with rocksalt-type structures propose two possibilities to make this face stable: (1) the bulk-terminated {111} surface facets into neutral {100}-type faces upon annealing or (2) the surface reconstructs.⁶ These two possibilities are similar, since the reconstruction can be considered as faceting on an atomic scale. Results obtained for NiO(111) in vacuum confirmed these predictions.⁷

In the case of growth from solution, recent work carried out in our group using formamide or CdCl₂ as impurities⁸ has shown that no reconstruction or faceting occurs for {111} NaCl surfaces. For the CdCl₂ case, it was concluded that the

surface is Cl⁻ terminated and that a disordered layer containing $\frac{1}{4}$ ML Cd²⁺ and $\frac{3}{4}$ ML H₂O stabilizes this surface.

For the formamide case, atomic force microscopy (AFM) and optical microscopy observations were not sufficient to determine the mechanism behind the stabilization. Therefore, we here report a surface x-ray diffraction investigation. Given the known difference in stability of the {111} face in water or formamide solutions, we expected large differences in the interface structure, but this turns out not to be the case. Instead, the formation of an electrochemical double layer is the main stabilizing mechanism in both cases.

II. EXPERIMENTAL PROCEDURE

The surface x-ray diffraction (SXR) technique is very suitable for the structure determination of the interface between a crystal surface and solution.⁹ In SXR, diffracted x-ray intensities along the so-called crystal truncation rods are measured.¹⁰ These rods are tails of diffuse intensity connecting the bulk Bragg peaks in the direction perpendicular to the surface. Their exact shape is determined by the atomic structure of the solid-liquid interface.

The octahedral NaCl crystals, with dimensions 4 × 4 × 3 mm³, were grown at our laboratory from supersaturated aqueous solution in the presence of formamide.³ After separation from the growth solution, the crystals were quickly dried using a paper tissue. AFM was used to check the surface prior to x-ray diffraction. Using AFM we found the {111} NaCl surface to be atomically smooth and covered with steps of height d_{111} , which means that the surface is either Cl⁻ or Na⁺ terminated.³ The surface patterns did not change when the crystals were kept dry in a desiccator.

The SXR experiments were performed at the DUBBLE and ID03 beam lines of the European Synchrotron Radiation Facility (ESRF) in Grenoble, using an x-ray energy of 10 keV. The data were collected under two different environmental conditions, namely by exposing the crystal surface (i) to 75% relative humidity (RH) and (ii) to forma-

^{a)}Author to whom correspondence should be addressed. Fax: +31 24-365-3067. Electronic mail: e.vlieg@science.ru.nl

vide vapor in a dry nitrogen atmosphere. The resulting thin solution layers lead to a much better signal-to-noise ratio than obtained for thicker films. The experiments were carried out at room temperature. The addition of 30% formamide to an aqueous solution is sufficient to stabilize the {111} face,³ but in these vapor pressure experiments we used pure vapors in order to have an unambiguous composition of the liquid film. The experimental setup consists of a cell in which the crystal surface can be examined in a well-controlled atmosphere.¹¹ This cell is coupled to a (2+3) diffractometer¹² operating in a vertical geometry in the case of the DUBBLE beam line and to a horizontal Z-axis diffractometer¹³ in the case of ID03. To establish equilibrium between crystal and vapor, the system was left for at least 15 min before every measurement.

In order to describe the NaCl {111} surface lattice and to index the x-ray reflections, we use a (111) surface unit cell. The lattice vectors \mathbf{a}_1 of this cell are expressed in terms of the conventional cubic lattice vectors by

$$\mathbf{a}_1 = \frac{1}{2}[10\bar{1}]_{\text{cubic}}, \quad \mathbf{a}_2 = \frac{1}{2}[\bar{1}10]_{\text{cubic}}, \quad \mathbf{a}_3 = [111]_{\text{cubic}},$$

with

$$|\mathbf{a}_1| = |\mathbf{a}_2| = \frac{1}{2}a\sqrt{2}, \quad |\mathbf{a}_3| = a\sqrt{3},$$

where $a=0.563$ nm is the lattice constant of NaCl. The corresponding reciprocal lattice vectors \mathbf{b}_j are defined by $\mathbf{a}_i \cdot \mathbf{b}_j = 2\pi\delta_{ij}$. The momentum transfer vector is given by $\mathbf{Q} = h\mathbf{b}_1 + k\mathbf{b}_2 + l\mathbf{b}_3$, with (hkl) as the diffraction indices. With our choice of the surface unit cell the index l corresponds with the direction perpendicular to the surface.

The integrated intensities of the (hkl) reflections were measured using rocking scans. They are converted into structure factor amplitudes by applying the appropriate geometrical and resolution corrections.¹⁴ This correction procedure puts all rods on the same relative scale, except for the specular data. The negative values for the diffraction index l are obtained by inverting the structure factors according to Friedel's rule. The parameters describing the different models are fitted to experimental structure factors using a χ^2 minimization. Model calculations and fitting are done using the ROD program.¹⁵

III. RESULTS

A. Solution layer thickness

The interface structure we measure is only representative of the situation during solution growth if the liquid layer is sufficiently thick. We therefore first determined this thickness by measuring the Kiessig fringes in the specular rod.¹⁶ We observed these fringes for both the water and the formamide atmosphere. Note that this confirms with high sensitivity earlier results using ellipsometry about the presence of such a layer.¹⁷ The measured layer thicknesses were completely reproducible at both beam lines. We could observe the evolution of the liquid layer thickness after the crystal was exposed to either water or formamide vapor. Figure 1 shows this for a case in which the crystal is exposed to the vapor pressure of a saturated NaCl solution in which

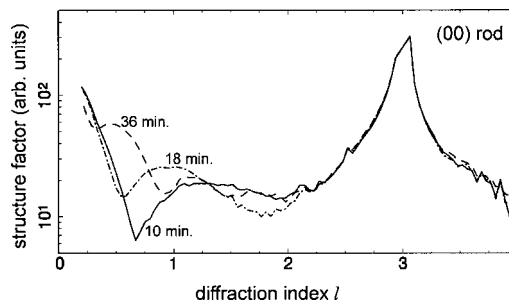


FIG. 1. The (00) rod measured after exposure of the {111} NaCl surface to the vapor pressure of a saturated NaCl solution in which 50 wt % formamide was added. The first Kiessig fringe can be seen at $l=1.1$ after 10 min (black solid line), at $l=0.9$ after 18 min (dot-dashed line), and at $l=0.5$ after 36 min (dashed line). For $l > 2.2$, no changes in the rod occur.

50 wt % formamide was added. In this case the measured layer thickness increases from 9 Å after 10 min of exposure to approximately 40 Å after 50 min.

In order to obtain a pure aqueous film, we inserted a NaCl-saturated solution in the sample cell, which gives a RH of 75%. This yields a stable layer with a thickness of 30 Å after 35 min. In the formamide case we derived a stable layer thickness of 24 Å from the Kiessig fringes. For both conditions we obtain a film that is sufficiently thick to obtain the equilibrium structure at the solid-liquid interface. This is confirmed by the fact that the specular rod is constant in time except for the part at low l .

B. Data set and model

For both environmental conditions more than 100 non-equivalent reflections were measured. The agreement factors are 7% in both cases, when averaged over equivalent reflections for all specimens used in each type of experiment. The data set consists of the (00), (10), and (20) rods; the results are shown in Fig. 2. The specular, or (00), rod gives information about the electron density perpendicular to the surface, whereas the two other rods are sensitive to in-plane ordering as well. The (00) rod shows the largest differences between the two environmental conditions, for the other rods the differences are surprisingly small, given the fact that the {111} face is thought to be unstable in water. We conclude that the interface structure is almost the same for the two environmental conditions. From the fact that the (20) rod, which is the least sensitive to the liquid structure, follows the profile expected for a bulk-terminated crystal, we further conclude that no reconstruction of the crystal occurs. This agrees with our AFM data.³

In order to fit the data, we need a model that describes the entire interface. Since our data set is limited, we further need to keep our model as simple as possible. We do not know the liquid structure *a priori* and therefore start with a generic model in which the amount of charge density at various lattice positions can be optimized. In this way we find that we need a strong contribution exactly located at a bulk-extrapolated fcc position on top of a Na-terminated surface, for both experimental conditions. The density corresponds to approximately 0.5 ML Cl. We find little difference between water and formamide, thus we do not locate the formamide

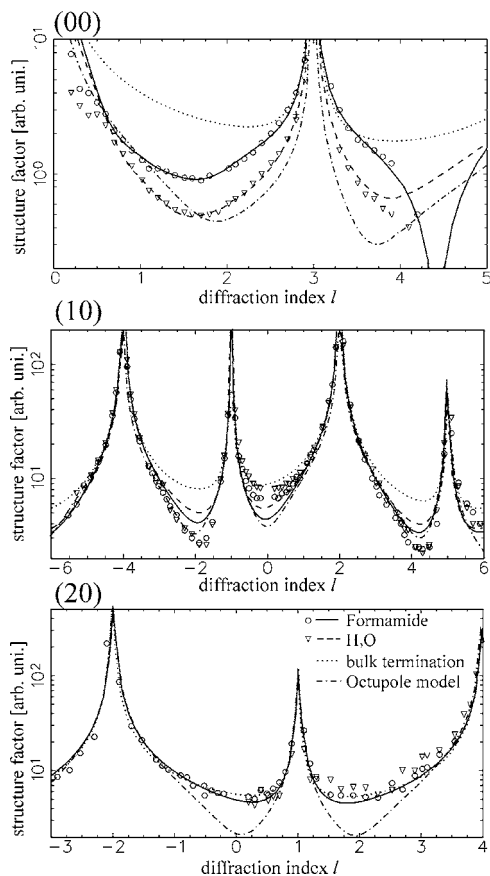


FIG. 2. Structure factor amplitude along the (00), (10), and (20) rods. Measured structure factors are indicated by symbols. The solid curve represents the best fit for formamide, the dashed curve is for water, the dotted curve is for a bulk-terminated crystal, and the dot-dashed curve represents the octupole model.

directly. While we initially expected to find a well-ordered formamide layer that would in this way stabilize the {111} surface, these results imply that we have to change our point of view. The data tell us that the interface consists of a bulk-terminated crystal with approximately 0.5 ML Cl on top. As will be explained fully in the Discussion section, this is an excellent way to obtain charge neutrality.

Based on this we can construct our final model, in which we add partially ordered liquid layers further away from the crystal (see Fig. 3). These water or formamide layers were modeled using only oxygen atoms, since x rays are insensitive to hydrogen and do not differentiate between O, N, and C at our precision level. For the crystal part we started with a bulk truncated {111} NaCl surface with a Na^+ layer on top. Above it we placed one Cl^- layer and two oxygen layers (O1 and O2). The various degrees of ordering in the liquid layers are modeled using anisotropic Debye-Waller and occupancy parameters. We find no lateral ordering in the layers O1 and O2, so the lateral Debye-Waller parameter for these layers is fixed at $B_{\parallel} = 1000 \text{ \AA}^2$. The top three layers can relax in the direction perpendicular to the surface. In first instance, we tested the model allowing also in-plane relaxations of the Cl^- layer. As the best fits were for a fcc site, we fixed the in-plane coordinates for this position in the final calculations. Similarly, we found no relaxation on the top Na^+ layer and fixed its position to the bulk value. The Debye-Waller,

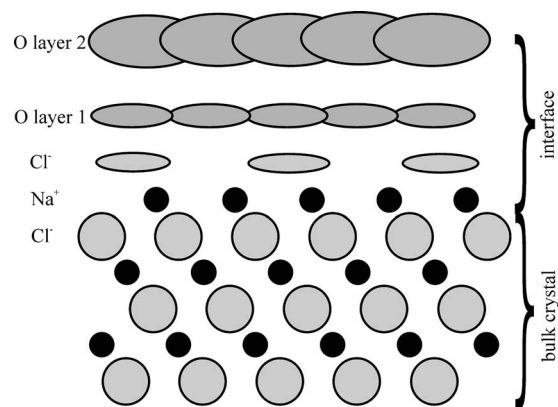


FIG. 3. Schematic side view of the {111} NaCl face used for modeling of the humid and formamide environments.

z -position, and occupancy parameters of the top Na^+ ion and the Cl^- and liquid layers were optimized during the fitting procedure.

For each environmental condition all rods were fitted simultaneously. We used the same model for the humid and formamide environments, which makes comparison simpler. Using this model, we obtained not perfect, but physically satisfactory fits of the experimental data for the humid and the formamide conditions with χ^2 values of 3 and 5, respectively. The best fitting parameters are listed in Table I and the fits are shown in Fig. 2. We can improve our fits slightly by adding more components to the model, e.g., allowing Cl^- to occupy both fcc and hcp positions, but given the limited size of our data set we restrict our model to the most important features. Models with Cl^- termination do not yield a satisfactory fit, showing that the {111} NaCl surface is Na^+ terminated for our experimental conditions.

C. Electron density distribution

A convenient way to visualize the liquid order adjacent to the crystal surface is to use a projection of the electron

TABLE I. Best fit parameters for the formamide and water environments. Values with an asterisk were fixed during fitting. The z positions are given with respect to an unrelaxed Cl^- top layer

Atom	Parameter	Formamide	Water
O2	z [\AA]	7.5(4)	4(2)
	B_{\parallel} [\AA^2]	1000*	1000*
	B_{\perp} [\AA^2]	1100(200)	1100(200)
	Occupancy	1.5(4)	2.0(7)
O1	z [\AA]	3.4(2)	2.0(5)
	B_{\parallel} [\AA^2]	1000*	1000*
	B_{\perp} [\AA^2]	141(80)	164(80)
	Occupancy	1.3(3)	1.0(5)
Cl^-	z [\AA]	-0.04(3)	-0.04(3)
	B_{\parallel} [\AA^2]	71(10)	86(10)
	B_{\perp} [\AA^2]	7(4)	7(9)
	Occupancy	0.4-0.7	0.4-0.7
Na^+	B [\AA^2]	0.4*	0.4*
	Occupancy	0.7-1.0	0.7-1.0
	χ^2	3.0	5.0

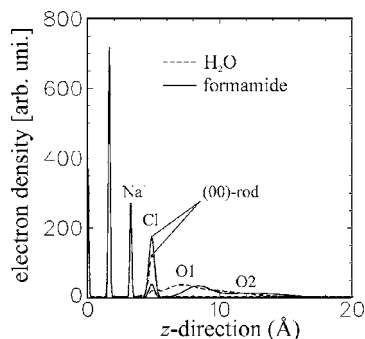


FIG. 4. Electron density distribution across the interface for the (a) formamide (solid line) and (b) humid circumstances (dotted line). The electron density distribution is shown for two parallel momentum transfers: (00) (two highest peaks) and (10) (two small peaks).

density on the z axis in which the effective density depends on the in-plane Debye-Waller parameter B_{\parallel} .¹⁸ The electron density distribution $\rho(z)$ is calculated by summing all the individual contributions of atoms using

$$\rho_z = \sum_i Z_i n_i \exp\left(-Q_{\parallel,i}^2 \frac{B_{\parallel,i}}{16\pi^2}\right) \times \frac{1}{\sqrt{2\pi\langle u_{\perp,i}^2 \rangle}} \exp\left(-\frac{(z_i - z)^2}{2\langle u_{\perp,i}^2 \rangle}\right), \quad (1)$$

where Z_i is the atomic number, n_i is the occupancy, $Q_{\parallel,i}$ is the parallel momentum transfer, $B_{\parallel,i}$ is the in-plane Debye-Waller factor, and z_i is the position of atom i . The mean vibration amplitude perpendicular to the plane is given by $\langle u_{\perp,i}^2 \rangle$ and is related to the out-of-plane Debye-Waller factor by $B_{\perp,i} = 8\pi^2\langle u_{\perp,i}^2 \rangle$. The first exponential term in Eq. (1) depends on the parallel momentum transfer and shows to which extent the different rods are sensitive to the liquid structure.¹⁸ This factor is equal to 1 for the specular rod (where $Q_{\parallel}=0$) and decreases for the other rods. For the specular rod all layers contribute, but for high in-plane momentum transfer only layers with sufficient lateral order are visible.

The calculated electron density distributions across the interface for both the water and formamide cases are shown in Fig. 4. The peak labeled Na^+ is the topmost crystal layer; its occupancy is found to lie between 0.7 and 1.0. On the liquid side we find one well-defined Cl^- layer on a fcc position for both the humid and the formamide atmosphere conditions. The in-plane Debye-Waller parameters show that this layer and the layers above are liquidlike; their contribution to the (10) rod is small. The occupancy of the Cl^- layer lies between 0.4 and 0.7 for both the formamide and the humid conditions. All these suggest a strong interaction of these chloride ions from the liquid side with the atoms of the topmost Na^+ crystal layer. The next liquid layers (modeled by oxygen atoms O1 and O2 in Fig. 4) show only out-of-plane ordering. Subsequent layers have no order and correspond to the disordered bulk liquid.

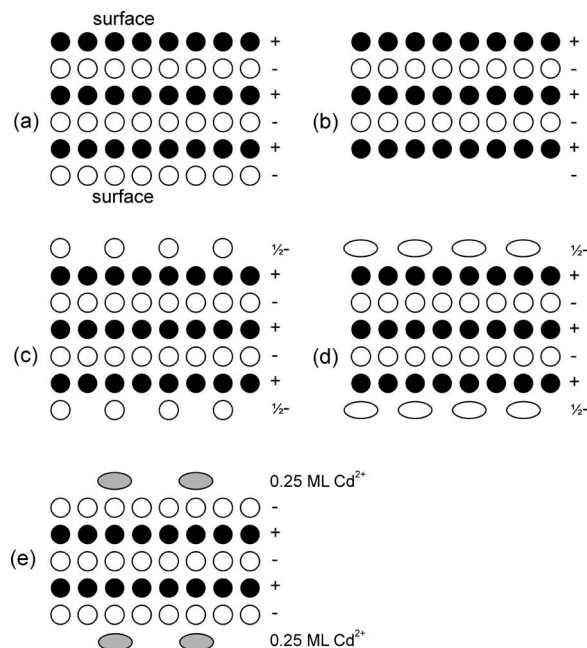


FIG. 5. Charge distribution vs stability of the polar $\text{NaCl}\{111\}$ surface. (a) The crystal is charge neutral, but its top and bottom surfaces have different terminations. (b) The terminations of the opposite surfaces are the same, but the crystal is charged and has a very high electrostatic energy. (c) By placing 0.5 ML Cl^- layer on top of the complete Na^+ layer for both sides, the crystal is both charge neutral and has the same termination on both sides. (d) Same as (c) but now the charge-compensating layer is part of the liquid. (e) For the CdCl_2 additive one has 0.25 ML Cd^{2+} on top of a complete layer of Cl^- . Also in this case the crystal is charge neutral and has the same termination on both sides.

IV. DISCUSSION

A. Surface structure

Our SXR D observations confirm the conclusion already drawn from the AFM measurements,³ that the $\text{NaCl}\{111\}$ surface is smooth at an atomic level and is not reconstructed. This supports the conclusion drawn by Brunsteiner and Price from their molecular dynamics simulation of $\{111\}$ potash alum in contact with a saturated aqueous solution that an electrostatically polar surface of an ionic crystal does not need to be reconstructed to be stable.¹⁹

As we previously mentioned, $\{111\}$ NaCl is a charged (polar) surface, where the topmost layer consists of either Na^+ or Cl^- ions. Our SXR D results show that the $\{111\}$ NaCl surface in the presence of formamide and water is Na^+ terminated and not reconstructed. Given these observations, a simple way to obtain charge neutrality is explained in Fig. 5. Consider a very thin NaCl crystal with top and bottom $\{111\}$ surfaces. This can be made charge neutral by having the same number of Na^+ and Cl^- layers, but then the top and bottom surfaces have a different termination [see Fig. 5(a)]. On thick crystals one observes only one type of termination, so this situation is unlikely. One can generate the same termination on both sides by removing one layer, but then the system is no longer neutral and will have a high electrostatic energy [see Fig. 5(b)]. By moving half a surface layer to the opposite side, finally, one can obtain a system that is both charge neutral and has the same structure on both sides [see Fig. 5(c)]. Other neutral surfaces are possible, because if one

removes (on both sides) the same amount of ions from the first and second layers of Fig. 5(c), charge neutrality is maintained.²⁰ The specific case of a top layer with 0.25 ML and a second layer with 0.75 ML corresponds to the octupole reconstruction model proposed by Lacmann.²¹ From our data we know that the surface is, however, *not* reconstructed. Figure 2 shows a calculation for this octupole model: the difference with the data is especially large for the (20) rod.

Our SXRD results show one well defined but weakly ordered Cl⁻ layer for both the humid and the formamide atmosphere conditions. The occupancy of this disordered and liquidlike layer (0.4–0.7) agrees with the 0.5 ML described in Fig. 5(c). Our data show that the charge-compensating Cl⁻ layer is not part of the crystal, but is part of the liquid. What we observe is, in fact, the diffuse half of the electrical double layer adjacent to the bulk truncated {111} Na⁺ terminated surface! This situation is sketched in Fig. 5(d). Unfortunately, we cannot determine the occupancy parameter very precisely. An occupancy larger than 0.5 can be explained by the fact that the first liquid layer also contains formamide or water molecules. Since the first layer is located exactly at an extrapolated Cl⁻ position, Cl⁻ indeed has to be a main component in this layer. The uncertainty in the occupancy of the topmost Na⁺ layer is also quite large (0.7–1.0). It is possible that the layer is fully occupied, as our earlier AFM observations suggest, but some vacancies could be present. A value of 0.75 corresponds to the value for the octupole model. This would imply a Cl⁻ occupancy of 0.25, which is within our fitted range when taking into account that in that case ~0.75 ML of water/formamide (with roughly half the charge density) needs to be added to the layer.

We find that the electrical double layer is very thin, only 5 Å for both conditions. This agrees with estimates using Grahame's equation²² for the present case. The analytical approach of calculating the properties of the electrical double layer on top of a NaCl {111} surface is described in Ref. 8. The calculations further show that about 80% of the charge-compensating Cl⁻ ions are confined to the first liquid layer.

The model indicates that for both pure water and formamide solutions, the main mechanism for stabilization is the compensation of the net charge of 0.5e⁺ per surface atom by the opposite charge of 0.5 ML of Cl⁻ in the first layer of the solution. This model can be extended to the case of Cd²⁺ impurities, which also leads to a crystal morphology with {111} faces.²³ Because of the double charge of the Cd²⁺ ions, one expects for that case 0.25 ML Cd²⁺ on top of a full Cl⁻ layer [see Fig. 5(e)]. This fully agrees with the results we obtained recently on that system.⁸

B. Stabilization of the {111} face

We have found that in both aqueous and formamide solutions, the solid-liquid structures are nearly the same and that in both cases, half a monolayer of Cl⁻ ions stabilizes the polar {111} surface. This means, however, that we have not yet explained the dramatic change in crystal morphology from {100} to {111} which occurs when formamide is added to a pure aqueous NaCl solution. The original explanation that the {111} face is not stable in water is found to be incor-

rect. So, there must be a (somewhat more subtle) difference in stability of both forms, such that the balance with respect to the {100} face changes when formamide is added. This must be related to the difference in the interaction of formamide and water with the interface.

Commonly, formamide and water are regarded as similar solvents, characterized by a large dielectric constant ($\epsilon = 109.5$ for formamide and 78.36 for water), a large dipole moment ($\mu = 3.37$ D for formamide and 1.84 D for water), and the formation of a three-dimensional hydrogen-bonded network. Molecular dynamics simulations of Na⁺ and Cl⁻ ion solvation in aqueous mixtures of formamide²⁴ as well as NMR measurements²⁵ show that the formamide molecules interact more strongly with the Cl⁻ and Na⁺ ions than the water molecules in forming a solvation shell. This suggests that the role of the formamide molecules in the stronger stabilization of the {111} NaCl surface compared to water could be the interaction with the first liquid Cl⁻ layer. This stabilizing interaction is stronger for formamide than for water, and thus results in the appearance and stability of octahedral {111} NaCl crystals. This agrees with Fig. 4, where the first liquid layer is more intense and better ordered for the formamide case. Another possible factor, which unfortunately cannot be verified by SXRD, is a difference in step structure and step energy for the two cases, which may also contribute to the observed difference in surface stability. More insight into the stabilization mechanism could come from molecular dynamics simulations of the interface, but these are challenging and reliable potentials are difficult to obtain.²⁶

Given the structural similarity between urea and formamide, it is likely that the explanation for the {111} morphology in the presence of urea is similar. We thus propose that also in the case of the classic observation of Rome de l'Isle² the {111} surface is flat and unreconstructed. Its presence in the morphology arises from the increased stability of the {111} interface thanks to the interactions of the urea with the first Cl⁻ layer in the liquid. Similar to formamide, we do not expect that urea is strongly bonded to the surface. This disagrees with the suggestion by Palm and MacGillavry²⁷ that an epitaxial NaCl-urea-H₂O compound forms on the {111} face. We have no direct data for the urea case, but we know that such an epitaxial layer is not present when formamide or CdCl₂ are used as additives.⁸

We find that for the cases of pure water solutions, and for formamide or Cd²⁺ additives, the main stabilization mechanism is the formation of a charge-compensating layer in the liquid, i.e., the formation of an electrochemical double layer. For charged surfaces in solution, this may be a common mechanism, because typically there are several ionic species present in the solution. For surfaces in vacuum, nature does not have this route available to minimize the surface energy. For {111} surfaces of crystals with the rocksalt structure in vacuum, indeed reconstructions have been found.⁷ Yet another means to obtain charge neutrality was reported for triangular (111) bulk-terminated NaCl islands grown in vacuum by adsorption of Na or Cl on Al(111) and Al(100). In that case the charge of the topmost layers differs from the bulk, and the islands were found to consist of two +1/2 charged Na layers with a Cl⁻ layer in between.²⁸

The large changes in morphology for NaCl as a function of additives are not apparent from the interface structure, but this is certainly not always the case. For example, for the {101} surfaces of potassium dihydrogen phosphate (KDP), the changes in growth velocity as a function of pH correspond with large changes in the interface structure.²⁹

V. CONCLUSIONS

By using surface x-ray diffraction, we have found that the main stabilizing mechanism for the polar {111} faces of NaCl in solution is the formation of a charge-compensating ion layer in the first liquid monolayer of the solution on top of an unreconstructed crystal surface. This also holds for pure aqueous solutions, and therefore the change in crystal morphology from {100} to {111} upon addition of impurities (formamide or Cd²⁺) arises from interactions in the liquid that are not directly visible in the interface structure. To achieve stabilization, nature thus chooses the formation of an electrochemical double layer. In vacuum this route is not available, and under these conditions a surface reconstruction or charge transfer is the only way to obtain a stable {111} surface on crystals with a rocksalt structure.

ACKNOWLEDGMENTS

The authors would like to thank the staff of the beam lines DUBBLE and the ID03 at the European Synchrotron Radiation Facility in Grenoble, France for their kind assistance during the measurements. Special thanks are given to Christophe Pelletier for inspiring discussions. This work is supported by the Council for Chemical Sciences of the Netherlands Organisation for Scientific Research (CW-NWO)

¹H. E. Buckley, *Crystal Growth* (Wiley, New York, 1951); J. Nyvlt and J. Ulrich, *Admixtures in Crystallization* (VCH, Weinheim, 1995); L. Lian, K. Tsukamoto, and I. Sunagawa, *J. Cryst. Growth* **99**, 150 (1990).

²J. B. L. Rome de l'Isle, *Cristallographie* (De l'Imprimerie de Monsieur, Paris, 1783).

³N. Radenovic, W. J. P. van Enkevort, P. Verwer, and E. Vlieg, *Surf. Sci.* **523**, 307 (2003).

⁴N. Radenovic, W. J. P. van Enkevort, and E. Vlieg, *J. Cryst. Growth*

263, 544 (2004).

⁵P. W. Tasker, *Philos. Mag. A* **39**, 119 (1975).

⁶A. Gibson, R. Haydock, and J. P. LaFemina, *J. Vac. Sci. Technol. A* **10**, 2361 (1992).

⁷M. A. Langell, C. L. Berrie, M. H. Nassir, and K. W. Wulser, *Surf. Sci.* **320**, 25 (1994); P. A. Cox and A. A. Williams, *ibid.* **152/153**, 791 (1985); N. Floquet and L. C. Dufour, *ibid.* **126**, 543 (1983); C. A. Ventrice, Jr., T. Bertrams, H. Hannemann, A. Brodde, and H. Neddermeyer, *Phys. Rev. B* **49**, 5773 (1994); H. Hannemann, C. A. Ventrice, T. Bertrams, A. Brodde, and H. Neddermeyer, *Phys. Status Solidi A* **146**, 289 (1994).

⁸N. Radenovic, W. J. P. van Enkevort, D. Kaminski, M. Heijna, and E. Vlieg, *Surf. Sci.* **599**, 196 (2005).

⁹E. Vlieg, *Surf. Sci.* **500**, 458 (2002).

¹⁰I. K. Robinson, *Phys. Rev. B* **33**, 3830 (1986).

¹¹J. Arsic, D. Kaminski, N. Radenovic, P. Poodt, S. Graswinckel, H. M. Cuppen, and E. Vlieg, *J. Chem. Phys.* **120**, 9720 (2004).

¹²E. Vlieg, *J. Appl. Crystallogr.* **31**, 198 (1998).

¹³J. Bloch, *J. Appl. Crystallogr.* **18**, 33 (1985).

¹⁴E. Vlieg, *J. Appl. Crystallogr.* **30**, 532 (1997).

¹⁵E. Vlieg, *J. Appl. Crystallogr.* **33**, 401 (2000).

¹⁶H. Kiessig, *Ann. Phys.* **10**, 769 (1931).

¹⁷J. H. Frazer, *Phys. Rev.* **34**, 644 (1929); W. Bayh and H. Pflug, *Z. Angew. Phys.* **25**, 358 (1968).

¹⁸M. F. Reedijk, J. Arsic, F. F. A. Hollander, S. A. de Vries, and E. Vlieg, *Phys. Rev. Lett.* **90**, 066103 (2003).

¹⁹M. Brunsteiner and S. L. Price, *J. Phys. Chem. B* **108**, 12537 (2004).

²⁰The general condition for having both charge neutrality and an identical structure on the opposite {111} faces is given by $2Sq_i n_i = \pm 1$. Here i is the surface layer number, starting from a fully occupied Na⁺ ($\Sigma = -1$) or Cl⁻ layer ($\Sigma = +1$), and q_i and n_i are the ion charge and occupancy of the ions in this layer. For instance, for the octupole model $q_1 = -1$, $n_1 = 3/4$, $q_2 = 1$, $n_2 = 1/4$, and $n_{i>2} = 0$.

²¹R. Lacmann, *Adsorption et Croissance Cristalline* (Centre National de la Recherche Scientifique, Paris, 1965).

²²D. C. Grahame, *J. Chem. Phys.* **21**, 1054 (1953); J. Israelachvili, *Intermolecular and Surface Forces* (Academic, London, 1992).

²³M. Bienfait, R. Boistelle, and R. Kern, *Adsorption et Croissance Cristalline* (Centre National de la Recherche Scientifique, Paris, 1965).

²⁴Y. P. Puhovski and B. M. Rode, *Chem. Phys.* **222**, 43 (1997).

²⁵C. K. Finter and H. G. Hertz, *Z. Phys. Chem., Neue Folge* **148**, 75 (1986).

²⁶I. Okada, Y. Namiki, H. Uchida, M. Aizawa, and K. Itatani, *J. Mol. Liq.* **118**, 131 (2005).

²⁷J. H. Palm and C. H. MacGillavry, *Acta Crystallogr.* **16**, 963 (1963).

²⁸W. Hebenstreit, M. Schmid, J. Redinger, R. Podlucky, and P. Varga, *Phys. Rev. Lett.* **85**, 5376 (2000).

²⁹D. Kaminski, N. Radenovic, M. Deij, W. J. P. van Enkevort, and E. Vlieg, *Phys. Rev. B* **72**, 245404 (2005).